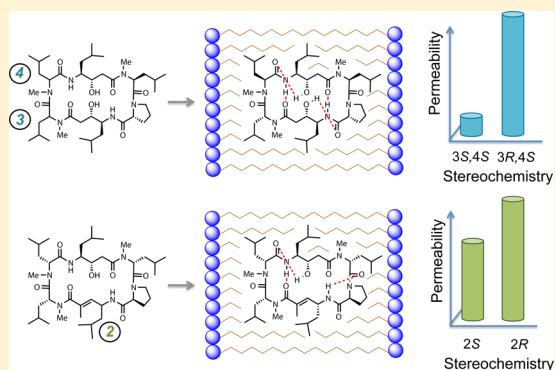


## Probing the Physicochemical Boundaries of Cell Permeability and Oral Bioavailability in Lipophilic Macrocycles Inspired by Natural Products

Andrew T. Bockus,<sup>†</sup> Katrina W. Lexa,<sup>‡</sup> Cameron R. Pye,<sup>†</sup> Amit S. Kalgutkar,<sup>§</sup> Jarret W. Gardner,<sup>†</sup> Kathryn C. R. Hund,<sup>†</sup> William M. Hewitt,<sup>†</sup> Joshua A. Schwochert,<sup>†</sup> Emerson Glassey,<sup>†</sup> David A. Price,<sup>||</sup> Alan M. Mathiowetz,<sup>||</sup> Spiros Liras,<sup>||</sup> Matthew P. Jacobson,<sup>\*,‡</sup> and R. Scott Lokey<sup>\*,†</sup><sup>†</sup>Department of Chemistry and Biochemistry, University of California—Santa Cruz, 1156 High Street, Santa Cruz, California 95064, United States<sup>‡</sup>Department of Pharmaceutical Chemistry, University of California— San Francisco, 1700 4th Street, San Francisco, California 94158, United States<sup>§</sup>Pharmacokinetics and Drug Metabolism, Pfizer Inc., Groton, Connecticut 06340, United States<sup>||</sup>Worldwide Medicinal Chemistry, Pfizer Inc., Groton, Connecticut 06340, United States

## Supporting Information

**ABSTRACT:** Cyclic peptide natural products contain a variety of conserved, nonproteinogenic structural elements such as D-amino acids and amide N-methylation. In addition, many cyclic peptides incorporate  $\gamma$ -amino acids and other elements derived from polyketide synthases. We hypothesized that the position and orientation of these extended backbone elements impact the ADME properties of these hybrid molecules, especially their ability to cross cell membranes and avoid metabolic degradation. Here we report the synthesis of cyclic hexapeptide diastereomers containing  $\gamma$ -amino acids (e.g., statines) and systematically investigate their structure–permeability relationships. These compounds were much more water-soluble and, in many cases, were both more membrane permeable and more stable to liver microsomes than a similar non-statine-containing derivative. Permeability correlated well with the extent of intramolecular hydrogen bonding observed in the solution structures determined in the low-dielectric solvent CDCl<sub>3</sub>, and one compound showed an oral bioavailability of 21% in rat. Thus, the incorporation of  $\gamma$ -amino acids offers a route to increase backbone diversity and improve ADME properties in cyclic peptide scaffolds.



## INTRODUCTION

The design of peptides with potent biological activity is a relatively straightforward undertaking when compared with the arduous task of converting lead peptides into drugs with favorable ADME properties. Although many effective peptide drugs have been brought to market, most of these are delivered parenterally against extracellular targets. Thus, the aphorism “Peptides do not make good drugs” continues to ring true with respect to achieving oral bioavailability and/or efficacy against intracellular targets. While cell-penetrating sequences such as Tat have garnered interest as delivery vehicles for a variety of bioactive peptide cargoes, after nearly 2 decades of research no such conjugates have been approved for clinical use, and their mechanism of cell penetration remains poorly understood.<sup>1</sup> On the other hand, some relatively large peptides, in particular cyclic peptide natural products such as cyclosporine A, can penetrate cells by passive diffusion and indeed have achieved clinical efficacy without the need for pendent permeabilizing

elements. These drugs raise the prospect of designing both bioactivity and permeability into the same molecule. However, predicting cell permeability and oral bioavailability in macrocyclic peptides poses challenges not faced with typical “rule-of-5” (Ro5) small molecules. This has motivated a number of recent studies by our group and others using synthetic model systems designed to tease out structure/property relationships in this traditionally “non-druglike” chemical space.<sup>2–4</sup> These molecules, while not bioactive in themselves, are designed to probe the physicochemical boundaries of this expanded chemical space within which passive cell permeability (and even oral bioavailability) can be achieved.

Macrocycles are larger and more complex than typical small molecule drugs, making them attractive scaffolds for tackling the growing list of more challenging therapeutic targets such as

Received: January 22, 2015

protein–protein interactions and other relatively flat binding surfaces.<sup>5–10</sup> Macrocycles, including many cyclic peptide natural products, tend to lie outside the guidelines for assessing druglikeness such as the Ro5<sup>11,12</sup> and yet can exhibit druglike passive membrane permeability and even, in some cases, oral bioavailability.<sup>4,13–15</sup>

Studies of small molecules have shown that passive membrane permeability is enhanced by the ability to adopt conformations that effectively shield polar groups from solvent, thus offsetting the free energy of desolvation and facilitating diffusion across the membrane.<sup>16–21</sup> The importance of conformation as a determinant of passive permeability has also been demonstrated in cyclic peptides, in which the shielding of polar backbone amides from solvent can be achieved either through intramolecular hydrogen bonding<sup>4,15,22–28</sup> or by steric occlusion.<sup>2,4</sup> The ability to access these lipophilic states is determined largely by the complex interrelationship between local backbone geometry and overall conformation, which, for cyclic peptides, is influenced by the ubiquitous presence of nonproteinogenic backbone elements such as D-amino acids, N-methylamides, and heterodetic (e.g., isopeptide) linkages. In addition, many peptide natural products (both linear and cyclic) also contain  $\gamma$ -amino acids, such as the statines found in didemnin B<sup>29</sup> (Figure 1) and spiruchostatin A<sup>30,31</sup> and the vinyllogous residues found in cyclotheonamide (Figure 1) and gallinamide A,<sup>32</sup> among others.<sup>33–36</sup>

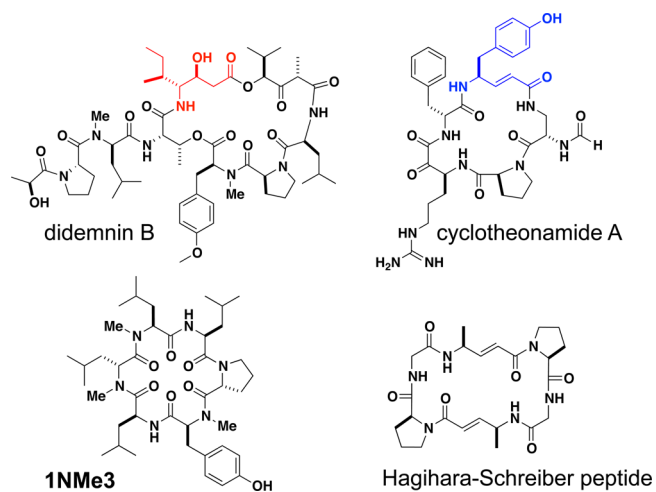


**Figure 1.** Didemnin B and cyclotheonamide A are bioactive macrocycles that contain polyketide-derived  $\gamma$ -amino acid residues. Compound 1NMe3<sup>15</sup> and the Hagihara–Schreiber peptide<sup>37</sup> are capable of adopting intramolecular hydrogen bonds and, along with the natural products, inspired the design of the scaffolds in this study.

While recent progress has been made in unraveling structure–permeability relationships in large macrocycles,<sup>38</sup> especially in cyclic peptides,<sup>4,24–26,39–48</sup> the extent to which these discoveries can be generalized to macrocycles containing non- $\alpha$ -amino acids remains largely unaddressed.

We hypothesized that, like the D- and N-methyl residues found in cyclic peptides, nonproteinogenic elements found in cyclic peptide–polyketide hybrids could influence membrane permeability through both local and global effects on backbone conformation. To investigate the impact of these moieties on the properties of cyclic peptides, we synthesized a small library of cyclic peptide diastereomers containing statine and vinyl-

ogous amino acids and studied their structural, physicochemical, and ADME properties. The resulting compounds, though similar to one another in sequence and composition, displayed a wide range of membrane permeabilities. We found that scaffold geometry could be optimized to generate highly permeable and, in one case, orally bioavailable macrocycles, allowing access to synthetic, beyond-Ro5 molecules with favorable PK properties and providing insights into the relationship between structure, conformation, and permeability in this underexplored chemical space.

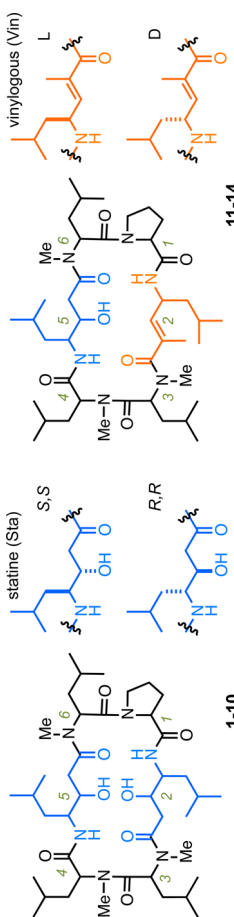
## RESULTS

**Selection of Compounds for Synthesis.** We generated a small library of cyclic peptides containing polyketide-inspired statine and vinyllogous residues flanked by turn-promoting dipeptide sequences (Table 1). On the basis of the published crystal structure of the Hagihara–Schreiber peptide,<sup>37</sup> containing similarly spaced vinyllogous amino acid residues (Figure 1), we predicted that this arrangement of  $\alpha$ - and  $\gamma$ -amino acids could allow, or enhance, the formation of internally hydrogen bonded conformations. Therefore, we synthesized two sets of diastereomers (Table 1), including matched pairs of epimers and enantiomers, in order to clarify the relationship between stereochemistry, conformation, and permeability in these hybrid macrocycles.

**Compound Synthesis.** The linear precursors of the 14 macrocycles in Table 1 were synthesized on the solid phase, followed by cyclization in solution. The amino acid building blocks were synthesized as their Fmoc-protected derivatives using published methods<sup>49–52</sup> and were coupled as typical amino acids without hydroxyl-group protection on 2-chlorotrityl polystyrene resin.<sup>52</sup> Macrocyces were determined to be  $\geq 95\%$  pure by LC–UV peak integration at 254 nm.

**Passive Membrane Permeabilities.** We investigated the passive membrane diffusion rates of the 14 hybrid macrocycles using the parallel artificial membrane permeability assay (PAMPA) system<sup>53</sup> and included propranolol as a known passively permeable and orally bioavailable control (Table 1). PAMPA is used to distinguish passive diffusion from active transport, and the resulting permeability values correlate well with in vivo absorption rates for drugs that cross the gut barrier by passive, transcellular diffusion.<sup>54</sup>

The library of 14 hybrid macrocycles demonstrated a wide range of permeabilities in a 5 h PAMPA incubation, consistent with previously established models relating passive permeability to conformation-dependent phenomena (e.g., the ability to form internal hydrogen bonds).<sup>15,17,21–23,26,47,48,55</sup> For comparison, we included the cyclic hexapeptide 1NMe3,<sup>15</sup> a cell-permeable and orally bioavailable compound that we discovered previously. Compounds 3, 6, 12, and 14 demonstrated excellent passive permeability, comparable to that of the propranolol control. Of the remaining compounds, 2, 4, 7, and 10 were more permeable than 1NMe3, and 1, 5, 8, 9 were less permeable than 1NMe3. As expected, the enantiomeric pair 8 and 9 showed similar permeabilities. Notably, some of the scaffolds containing two statines were no less permeable than scaffolds containing one statine and one vinyllogous residue. Compounds 9 and 13, which maintain identical stereochemistry but vary in monomer type at position 2, have similar PAMPA permeabilities. This observation is consistent with other reports showing that conformation can outweigh the effect of polar functionality in determining passive permeability and that three-dimensional structural models are

Table 1. Permeability and Physicochemical Properties of Scaffolds Containing Statine and Vinyllogous Residues at Positions 2 and 5<sup>f</sup>


compd	residue						PAMPA						solubility <sup>g</sup> PBS ( $\mu\text{M}$ )	eLogD <sup>h</sup>	EPSA <sup>i</sup>			
	1	2	3	4	5	6	MeLeu	MeLeu	Sta	MeLeu	$T^a$ (%)	$P_e^b$ ( $\times 10^{-6}$ cm s <sup>-1</sup> )				$R^d$ (%)	MDCK-LE $P_{app}$ ( $\times 10^{-6}$ cm s <sup>-1</sup> ) <sup>e</sup>	HLM CL <sub>int</sub> ( $\mu\text{g min}^{-1}$ mg <sup>-1</sup> ) <sup>f</sup>
1	D	S,S Sta	L	L	S,S	L	MeLeu	MeLeu	Sta	MeLeu	2 ± 1	1 ± 1	54	0.8 (3.3)	188	200	6.0	61
2	L	S,S Sta	L	L	S,S	L	MeLeu	MeLeu	Sta	MeLeu	28 ± 5	8 ± 2	56	3.6	183	*	5.7	55
3	D	R,R Sta	L	L	S,S	L	MeLeu	MeLeu	Sta	MeLeu	41 ± 5	12 ± 2	73					
4	D	S,S Sta	D	L	S,S	L	MeLeu	MeLeu	Sta	MeLeu	25 ± 1	7 ± 0	40	7.7 (4.2)	30	>600	6.9	57
5	D	S,S Sta	L	D	S,S	L	MeLeu	MeLeu	Sta	MeLeu	7 ± 1	2 ± 0	96	1.4 (1.3)	31	>600	6.1	62
6	D	S,S Sta	L	L	R,R	L	MeLeu	MeLeu	Sta	MeLeu	58 ± 5	20 ± 3	68	2.0 (9.0)	290	200	6.3	57
7	D	S,S Sta	L	L	S,S	D	MeLeu	MeLeu	Sta	MeLeu	24 ± 3	6 ± 1	92					
8	D	R,R Sta	L	L	R,R	L	MeLeu	MeLeu	Sta	MeLeu	16 ± 2	4 ± 1	26	5.7	142	*	*	61
9	I	S,S Sta	D	D	S,S	D	MeLeu	MeLeu	Sta	MeLeu	12 ± 4	3 ± 1	26					
10	D	S,S Sta	D	D	R,R	D	MeLeu	MeLeu	Sta	MeLeu	25 ± 1	7 ± 0	76					
11	I	L Vin	L	L	R,R	L	MeLeu	MeLeu	Sta	MeLeu	13 ± 3	3 ± 1	38					
12	I	D Vin	L	L	R,R	L	MeLeu	MeLeu	Sta	MeLeu	37 ± 5	11 ± 2	43	9.5 (10.1)	253	*	6.7	56
13	I	L Vin	D	D	S,S	D	MeLeu	MeLeu	Sta	MeLeu	11 ± 5	3 ± 1	21	11.2 (14.2)	45	>600	7.4	57
14	I	D Vin	D	D	S,S	D	MeLeu	MeLeu	Sta	MeLeu	35 ± 4	10 ± 1	34	11.2 (16.0)	216	>600	6.7	57
1NMe3 <sup>c</sup>											35	3		4.9	110	90	6.6	77
CSA											46 ± 4	14 ± 2		1.1	47			
propranolol														7.0				

<sup>a</sup>Values shown are averaged from at least four, at most eight, individual PAMPA measurements. Major outliers were removed from the data prior to calculation of %  $T$ . <sup>b</sup>Values shown are averaged from at least four, at most eight, individual PAMPA measurements. Major outliers were removed from the data prior to calculation of  $P_e$ . <sup>c</sup>16 h PAMPA (compound 3 in ref 15). <sup>d</sup>Percent recovery calculation in the Supporting Information. <sup>e</sup>In vitro permeability in low-efflux MDCK cell line (ref S6). Parenthetical data acquired in a low-binding assay (Supporting Information). Error does not exceed 20% based on internal controls. <sup>f</sup>Human liver microsome intrinsic clearance. <sup>g</sup>Kinetic solubility determined as described in Supporting Information. <sup>h</sup>eLogD data obtained as described in ref S8. <sup>i</sup>EPSA data obtained as described in refs 59 and 60. <sup>j</sup>The asterisk (\*) indicates that data were not acquired because of insufficient material.

Table 2. Rat Pharmacokinetics for 4, CSA, and INMe3

compd	intravenous administration				oral administration		
	AUC (ng h mL <sup>-1</sup> )	CL (mL min <sup>-1</sup> kg <sup>-1</sup> )	V <sub>dis</sub> (L kg <sup>-1</sup> )	t <sub>1/2</sub> (h)	AUC (ng h mL <sup>-1</sup> )	C <sub>max</sub> (ng mL <sup>-1</sup> )	F (%)
4 <sup>a</sup>	1697	10	1.1	1.6	1760	324	21
INMe3 <sup>b</sup>	3800	4.5	1.1	2.8	10500	852	28
CSA <sup>c</sup>	47600	3.5	1.2	6	13800	1440	29

<sup>a</sup>iv dose = 1 mg/kg; oral dose = 5 mg/kg; male Wistar–Han rats. Dosing vehicle: 10% propylene glycol, 5% Tween 80, 85% 20 mM sodium phosphate buffer. <sup>b</sup>iv dose = 1 mg/kg; oral dose = 10 mg/kg; male Wistar–Han rats. <sup>c</sup>iv and oral dose = 10 mg/kg.<sup>70</sup>

required to predict membrane permeability among compounds of similar composition.<sup>4,15,17,25,26,43,47,48</sup> Compounds 8 and 9, which had the poorest % recovery in the PAMPA assay (indicative of plate adherence or sequestration in the artificial membrane), also showed very low permeabilities, although poor PAMPA permeability did not necessarily correspond to low recovery (e.g., 5).

**In Vitro Cell Permeabilities.** A series of macrocycles representing a range of permeabilities, 1, 4, 5, 6, 7, 10, 12, 13, 14, was examined in a live-cell permeability assay that uses the Madin–Darby canine kidney low-efflux (MDCK-LE) cell line.<sup>15,56</sup> These cells were selected to express low levels of P-glycoprotein and provide a measure of passive transport with minimal interference from active efflux mechanisms. All compounds in this study displayed permeabilities comparable to or higher than that of the orally bioavailable cyclic peptide, cyclosporine A (CSA, Table 1). Compounds 1 and 5 showed relatively low MDCK-LE permeability, consistent with the PAMPA results for these compounds. Compound 6, which was the most permeable by PAMPA, initially showed low permeability in MDCK-LE cells, but when reassayed using coated plates to minimize nonspecific binding, this compound showed significantly higher permeability. We attributed the difference between the PAMPA permeability and the initial low MDCK-LE permeability to be the result of nonspecific adherence to the assay plates in the cell-based system. The other compounds containing two statines, 2, 4, and 10, demonstrated good permeability in both the PAMPA and MDCK-LE permeability assays. Although they displayed a range of permeabilities in PAMPA, the compounds that contained a vinylogous residue in place of one of the statines, 12, 13, and 14, were all remarkably permeable by MDCK-LE, with  $P_{app}$  values of  $9.5 \times 10^{-6}$  cm/s or greater.

**Microsomal Stability.** The MDCK-LE compounds were also tested for metabolic stability in vitro using human liver microsomes. Compounds 4, 5, and 13 demonstrated greater microsomal stability than both CSA and INMe3 (Table 1), while the others were less stable than either control. Consistent with previous observations with diastereomeric cyclic hexapeptides,<sup>15</sup> pairs of epimers showed different clearance rates (e.g., 1 vs 4; 13 vs 14).

**In Vivo Pharmacokinetic Studies.** Because of its favorable live-cell permeability and relatively low clearance in the liver microsome assay, we selected 4 for oral pharmacokinetics studies. Following an intravenous (iv) dose of 1.0 mg/kg to male Wistar–Han rats ( $n = 3$ ), compound 4 exhibited a low plasma clearance ( $CL_p$ ) of  $10.1 \pm 1.8$  mL min<sup>-1</sup> kg<sup>-1</sup> and a moderate steady state distribution volume ( $V_{dis}$ ) of  $1.05 \pm 0.12$  L/kg, which translated into an elimination half-life ( $t_{1/2}$ ) of  $1.55 \pm 0.06$  h (Table 2). Following oral (po) administration of 4 at 5.0 mg/kg to male Wistar–Han rats ( $n = 2$ ), systemic exposure of 4 as ascertained from the mean maximal plasma concentration ( $C_{max}$ ) and the mean area under the plasma

concentration–time curve from zero to infinity ( $AUC_{0-\infty}$ ) was 324 ng/mL and 1760 ng·h/mL, respectively. The corresponding oral  $F$  was ~21%. In summary, the pharmacokinetics of 4 in the rat were comparable to the parameters previously reported for INMe3<sup>15</sup> and CSA.<sup>57</sup> Concentration–time profiles for iv and po doses in rats are depicted in Figure S1.

**Physicochemical Properties.** To gain a better understanding of the relationship between discrete physicochemical properties and passive cell permeability, the solubility, effective log  $D$  (eLogD),<sup>58</sup> and EPSA<sup>59,60</sup> of the macrocycles with known MDCK-LE permeability were assessed. The solubility in phosphate buffered saline (PBS) was noticeably higher for compounds in this series relative to INMe3 (Table 1). The eLogD, an HPLC-based predictor of lipophilicity and octanol–water partitioning at pH 7.4,<sup>58</sup> indicated high lipophilicity for the extended macrocycles and correlated well with live-cell permeability (Figure 2). Compound 4 had a higher eLogD than

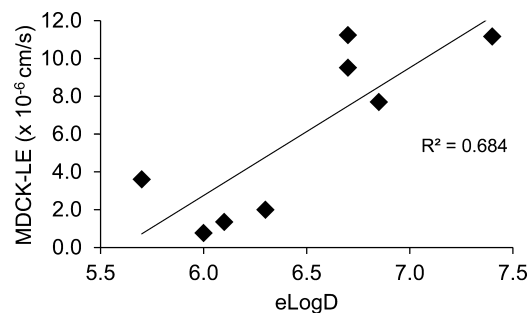
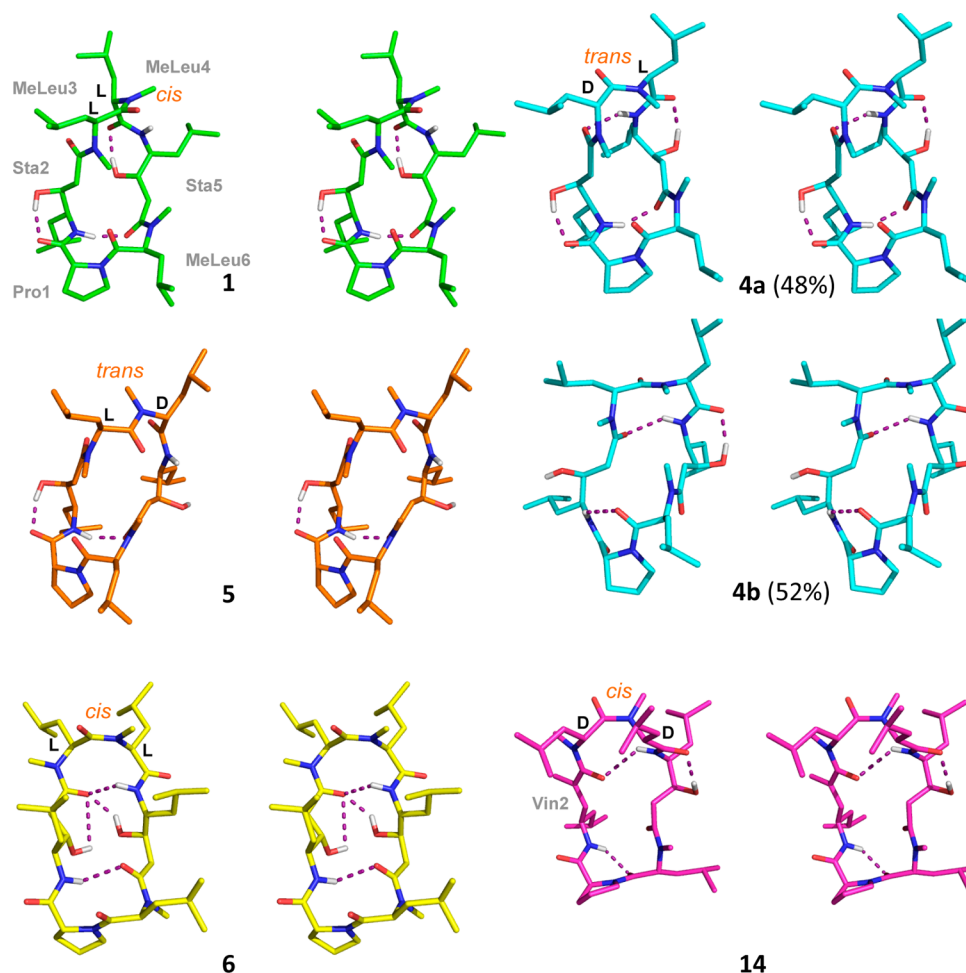


Figure 2. Live-cell permeability vs eLogD.

12 and 14, despite the presence of an additional hydroxyl in its backbone. EPSA, a supercritical fluid chromatography method that correlates retention with exposed polarity to identify intramolecular hydrogen-bonding and estimate polar surface area,<sup>59,60</sup> was also used to assess the scaffolds. All macrocycles assayed had EPSA values less than that of INMe3 (Table 1) and fell well under the 100 EPSA rule-of-thumb cutoff for permeable cyclic peptides.<sup>60</sup>

**NMR-Derived Solution Conformations.** On the basis of earlier studies with cyclic peptides of similar size,<sup>15,22,23,25</sup> we hypothesized that the wide range in permeabilities observed for 1–10 was related to differences in their ability to shield NH and/or OH groups in low-dielectric media, either sterically or through the formation of internally hydrogen bonded conformations. We used 2D NMR to investigate the solution conformations of four diastereomers in the statine series (1, 4, 5, and 6) and the vinylogous macrocycle, 14, in the low-dielectric solvent CDCl<sub>3</sub>. We used standard 2D NMR methods to assign all of the resonances in each compound and gathered NOESY cross-peak volumes and <sup>3</sup>J<sub>NH-H $\alpha$  coupling constants to obtain interproton distance<sup>61,62</sup> and dihedral information. In addition, <sup>13</sup>C chemical shifts of Pro carbons  $\beta$  and  $\gamma$  were used</sub>



**Figure 3.** NMR solution structures of compounds **1**, **4**, **5**, **6**, and **14** determined in  $\text{CDCl}_3$ . For **4**, multiple conformers were obtained as the best fit to the NOESY and  $^3J$  data. See **1** for residue assignments. Hydrogen bonds ( $<2.8$  Å) are shown in purple. Percentages refer to the DISCON conformer population contribution.

to ascertain the presence of *cis*-amides about the Pro  $\omega$ -torsions, and strong  $\text{H}\alpha$ -to- $\text{H}\alpha$  NOESY cross-peaks provided diagnostic evidence of *cis*-amides at some of the MeLeu positions. We sampled the conformations of **1**, **4**, **5**, **6**, and **14** using a computational algorithm that we had previously developed to predict loops in proteins<sup>63</sup> and modified to accommodate macrocycles.<sup>22</sup> Conformers within 5 kcal/mol of the global minimum for each structure were retained, clustered by backbone rmsd, and used as input into the “distribution of solution conformations” (DISCON)<sup>47,64,65</sup> algorithm, which fits NMR-derived distance and dihedral information to weighted ensembles of conformers rather than assuming a single well-defined conformer. In all but one case, DISCON yielded a single conformer as the best fit to the NOESY and  $J$ -coupling data (Figure 3 and Table S5). For **4**, the DISCON output with the lowest error was represented by an ensemble consisting of two conformers, **4a** and **4b**. These conformers differ primarily in a large rotation in the MeLeu3  $\varphi$  angle, resulting in a hydrogen bond shift of the neighboring statine’s NH from the C=O of the other statine at  $i + 3$  to form a  $\beta$ -turn, to that of the neighboring MeLeu at  $i + 2$  to form a  $\gamma$ -turn. In both structures of **4**, NH hydrogen bonding is maintained.

As expected, the solution structures showed varying degrees of polar atom solvent exposure, particularly for the amide NH groups while the participation of backbone OH groups in

intramolecular hydrogen bonds did not correlate strongly with permeability (Figure 3). The less permeable compounds, **1** and **5**, featured amides that were significantly solvent-exposed, while amides of the more permeable compounds **4**, **6**, and **14** showed very little solvent exposure. Despite their overall structural similarity, the solution structures showed a variety of conformations and intramolecular hydrogen bonding patterns (Figure 3). For example, compounds **1**, **6**, and **14** each contained one *cis*-amide, while the other compounds were all-*trans*.

We observed that compounds in which MeLeu3 and MeLeu4 have the same stereochemistry adopt a *cis* geometry at the MeLeu3-MeLeu4 amide, while compounds in which MeLeu3 and MeLeu4 have opposing configurations adopt a *trans* geometry (Figure 3, Table S3). For example, the L-MeLeu3-L-MeLeu4 amide in **1** is *cis*, while the D-MeLeu3-L-MeLeu4 amide in **4** is *trans* (the only difference between **1** and **4** being the configuration at MeLeu3). Compound **5**, which is also an epimer of **1**, contains the sequence L-MeLeu3-D-MeLeu4 and like **4** adopts a *trans* amide geometry. Similarly, **6** (L-MeLeu3-L-MeLeu4) and **14** (D-MeLeu3-D-MeLeu4), both with matching configurations, have *cis* amides at this position. However, the impact of *cis*–*trans* isomerism on global backbone conformation is not straightforward and depends on the pattern of stereocenters in the rest of the molecule.

Thus, there is in no direct correlation between the geometry about the MeLeu3–MeLeu4 amide bond and cell permeability in this series. For example, **4** is significantly more permeable than **5**, even though both compounds are all-*trans*. The sequence of stereocenters in **5** prevents the Sta5 NH from forming an intramolecular hydrogen bond, while the stereochemical arrangement of **4** allows it to adopt a classic  $\beta$ -turn about D-MeLeu3-L-MeLeu4, allowing for shielding of both NH groups in  $\beta$ -turns. Therefore, local geometric features like amide bond isomerism are context specific and do not translate directly to permeability because of the more global flexibility of the extended backbone. Nonetheless, the solution structures reveal that, in general, the NH hydrogen bond counts for cyclic peptides **1**, **4**, **5**, **6**, and **14** correlate well with cell permeability and EPSA, while hydrogen bonding among the –OH groups is prevalent throughout most of the structures and does not appear to correlate with permeability. These observations are consistent with other studies that challenge overall hydrogen bond count as a useful predictor of permeability,<sup>2,4,22,44</sup> especially when other factors are at play (such as flexibility and steric occlusion of polar groups).

## DISCUSSION

We have shown that extended amino acids can be incorporated into cyclic peptide scaffolds to yield macrocycles that preserve the permeability (and in one case the oral bioavailability) of the parent scaffold. These hydroxylated macrocycles maintain water solubility while remaining in a high-eLogD range and have lower EPSA than the parent compound **1NMe3**. The physicochemical properties of these hybrid scaffolds can be tuned to exhibit favorable ADME properties by manipulating the stereochemistry at single positions, and these local permutations drive the adoption of low energy conformations that afford permeation across biological membranes.

An ensemble of two conformers was identified as the best-fit NMR structure for compound **4**, possibly implying fast exchange between the two conformers. Though the backbone may be flexible, the structure shields the NH groups from solvent in both conformations. This flexibility observed by NMR in CDCl<sub>3</sub> may favor permeability by reducing the entropic penalty associated with adopting a single conformer in the low dielectric of the membrane. The ability of **4** to sample multiple internally hydrogen bonded conformers in fast exchange contrasts with the low dielectric conformation of CSA, which is assumed to be relatively rigid in its lipophilic state.<sup>28</sup> Alternatively, from a kinetic perspective flexibility could enhance permeability by allowing the molecule to adapt (through rapid conformational sampling) to the transitional environment at the water–lipid interface. It is possible, however, that the other macrocycles in this series could also exhibit flexibility, but limitations of the DISCON algorithm, NMR data, and/or conformational sampling resulted in the selection of a single conformer.

Permeabilities observed in passive diffusion and live-cell assays can be rationalized by considering the extent of NH hydrogen bonding in NMR-refined low-energy structures, supporting the hypothesis that hydrogen bonding plays a key role in determining the permeability of complex natural product-like scaffolds. But as we have seen in previous studies with cyclic hexa- and heptapeptides, intramolecular hydrogen bonding is, by itself, only weakly correlated with membrane permeability within a library of related scaffolds.<sup>22</sup>

Nearly all of the statine hydroxyls among the five compounds studied by solution NMR are involved in intramolecular hydrogen bonds, pointing toward the exposed NH groups, and not the hydroxyls, as the main factor influencing permeability within this series. Nonetheless,  $\beta$ -hydroxylation is common in natural products, as found in the structures of CSA,<sup>66,67</sup> aureobasidin A,<sup>67</sup> luzopeptin,<sup>68</sup> and guangomide A,<sup>69</sup> among many others. In a recent survey of the structures of macrocyclic ligands bound to their respective targets, such so-called “peripheral atoms” (non-hydrogen atoms directly attached to the macrocycle) were found to make up a disproportionately large percentage of the binding interface.<sup>10</sup> Our study shows that, at least in this series, the peripheral OH groups can be masked in the nonpolar environment of the membrane. Whether these groups would also be available to make productive contacts with a protein target (as in the case of CSA) remains a question for further investigation. This conformational flexibility may impart unique properties to these molecules, with the backbone hydroxyls leading to improved water solubility and microsomal clearance without compromising the ability to form highly lipophilic, membrane permeable conformers.

The vinylogous acid-containing compounds were on average more permeable than the all-statine compounds. The replacement of a statine residue with a vinylogue may permit facile permeation primarily by increasing relative hydrophobicity by stabilizing conformations with reduced NH solvent exposure, or by increasing rigidity, although the current study cannot deconvolute these effects.

We discovered a synthetic hybrid macrocycle, **4**, with desirable pharmacokinetic properties and good bioavailability after surveying no more than 6% of the 256 possible stereoisomers in this sequence alone. Compounds **6**, **12**, **13**, and **14** also demonstrated favorable druglike permeability in cell-based assays. It is therefore likely that many other permeable scaffolds exist even among other diastereomers in this narrowly defined series. The peptides studied here are, like CSA, characterized by mostly lipophilic side chains and represent only a small subset of all known bioactive peptides, most of which are relatively hydrophilic and not likely to be passively permeable. The class of passively permeable cyclic peptides is likely to grow as we understand more about the factors that govern the physicochemical and ADME properties of molecules in this space.

## EXPERIMENTAL SECTION

**General.** All macrocycles were confirmed to be  $\geq 95\%$  pure by HPLC. A detailed description of all materials and methods available in the Supporting Information.

**Macrocycle Synthesis and Purity.** Linear peptides were synthesized on 2-chlorotrityl resin using standard Fmoc coupling. The linear peptides were cleaved from resin with 1% TFA in DCM. Cyclization was performed in dilute conditions (<0.5 mg/mL peptide in a solution of 1:1 THF/ACN) with HOAT (3 equiv), PyBOP (3 equiv), and DIPEA (8 equiv), stirring overnight at room temperature. Compounds were purified by HPLC with mass-directed collection, and yields of purified cyclic product averaged  $12\% \pm 5\%$  based on initial resin loading. No dimers were detected in the mass range ( $m/z$  180–2000). Compounds **1**–**14** were confirmed to be  $\geq 95\%$  pure by LC–UV using a Thermo-Finnigan LCQ Classic equipped with a standard ESI ion trap and photodiode array detector. Samples were run on a reverse phase C18 column (HA 50 mm  $\times$  4.6 mm CS-0546-C158) with a 1.0 mL/min flow rate at ambient temperature using a mobile phase of acetonitrile–water containing 0.1% formic acid. The acetonitrile–water ratio was held at 50% for 2 min, then increased

linearly from 50% to 100% over 8 min, then held constant at 100% for an additional 2 min, and re-equilibrated to 50% for 2 min. Compound purity was determined by integrating peak areas of the liquid chromatogram, monitored at 254 nm.

**PAMPA Studies.** A 96-well filter plate with 0.45  $\mu\text{m}$  hydrophobic Immobilon-P membrane supports (Millipore) was loaded with an artificial lipid membrane composed of 1% lecithin in dodecane. Samples (10  $\mu\text{M}$ ) were run for 10 h at 25  $^{\circ}\text{C}$  and pH 7.4, and the concentration of compound in the donor and acceptor wells was quantified by LC–MS with an internal standard. Samples were run in triplicate against a propranolol standard.

**MDCK-LE Studies.** Samples were incubated for 2 h at 37  $^{\circ}\text{C}$  with MDCK-LE cells, in triplicate, against aliskiren and atenolol standards. LC–MS/MS was used to quantify the concentrations in the apical and basolateral compartments to calculate flux. Experiments were performed by Pfizer, Inc.

**Rat Pharmacokinetic Studies.** Compound 4 was administered intravenously to Wistar–Han rats ( $n = 3$ ) at 1 mg/kg as a solution in 10% propylene glycol/5% Tween 80/85% 20 mM sodium phosphate buffer (pH 7.4). Blood samples were collected at multiple time points after dosing. For oral studies, Wistar–Han rats were administered 4 at 5 mg/kg as a suspension in 25% PEG400/75% water. Serial blood samples were collected at multiple time points after dosing. Plasma aliquots were diluted 1:1 with acetonitrile/methanol containing terfenadine as an internal standard. The samples were vortexed and centrifuged, and supernatants were analyzed by LC–MS/MS to calculate the concentration of 4 by interpolation from a standard curve. Experiments were performed by BioDuro.

**Solubility.** DMSO stocks of compound (1  $\mu\text{L}$ , 60 mM) were added to 100  $\mu\text{L}$  of PBS (pH 7.4) and sonicated. The solution was incrementally diluted with PBS and sonicated until solid completely dissolved.

**NMR Studies.** All spectra were recorded on a Varian Inova 600 MHz spectrometer with a 5 mm inverse detection probe at 25  $^{\circ}\text{C}$ , unless otherwise specified. Chemical shifts were referenced to  $\text{CDCl}_3$  ( $\delta\text{H}$  7.26,  $\delta\text{C}$  77.16). Resonances for each amino acid residue was accomplished with  $^1\text{H}$ ,  $^{13}\text{C}$ , gCOSY, HSQC, HMBC, and TOCSY experiments. NOESY experiments were performed with a mixing time of 600 ms, d1 of 1.5 s, nt of 8, ni of 200, and ss of 32. NOESY correlations were documented for all available signals and converted to interproton distances. DISCON was used to fit the low-energy conformations (5 or 10 kcal/mol from the global minima) to the NMR data. 100 runs were performed for cluster levels between 1 and 20 to identify the relative contribution of each conformation to the NMR data. Clusters with the lowest total error were selected as the representative population ensemble for each compound.

## ■ ASSOCIATED CONTENT

### ■ Supporting Information

Synthesis and characterization details for amino acid monomers and cyclic peptides 1–14, methods for PAMPA and MDCK permeability, bioavailability, NMR structure determination, computational modeling, and NMR and LC–MS spectra. The Supporting Information is available free of charge on the ACS Publications website at DOI: 10.1021/acs.jmedchem.5b00128.

## ■ AUTHOR INFORMATION

### ■ Corresponding Authors

\*M.P.J.: e-mail, matt.jacobson@ucsf.edu; telephone, 415-514-9811.

\*R.S.L.: e-mail, slokey@ucsc.edu; telephone, 831-459-1307.

### ■ Notes

The authors declare the following competing financial interest(s): M.P.J. is a consultant to Pfizer and Schrodinger LLC, which licenses, develops, and distributes software used in

this work. M.P.J. and R.S.L. are founders of Circle Pharma, a macrocycle design company.

## ■ ACKNOWLEDGMENTS

A.T.B. would like to thank Dr. Hsiao-Wei Lee, Dr. Onur Atasoylu, Dr. Rushia Turner, Dr. Rebecca Braslau, Dr. Roger Linington, Vong Sok, Christopher Ahlbach, and Chad Townsend for helpful discussions. K.W.L. would like to thank GM100619 for support. The authors would also like to thank Dr. Gilles Goetz and Marina Shalaeva for generating the ElogD and EPSA data.

## ■ ABBREVIATIONS USED

PAMPA, parallel artificial membrane permeability assay; MDCK-LE, Madin–Darby canine kidney low efflux; THF, tetrahydrofuran; HOAT, *N*-[(dimethylamino)-1*H*-1,2,3-triazolo[4,5-*b*]pyridine-1-ylmethylene]-*N*-methylmethanaminium hexafluorophosphate *N*-oxide; PyBop, (benzotriazol-1-yloxy)tripyrrolidinophosphonium hexafluorophosphate; DIPEA, *N,N*-diisopropylethylamine;  $\text{CDCl}_3$ , deuterated chloroform; ACN, acetonitrile; DCM, dichloromethane; TFA, trifluoroacetic acid; CSA, cyclosporin A; NOESY, nuclear Overhauser effect spectroscopy; DISCON, distribution of solution conformations; Fmoc, fluorenylmethoxycarbonyl; ADME, absorption, distribution, metabolism, and excretion; PBS, phosphate buffered saline; CL, clearance; AUC, area under the curve;  $P_{\text{app}}$ , apparent permeability;  $P_e$ , effective permeability; Ro5, rule of five

## ■ REFERENCES

- (1) Copolovici, D. M.; Langel, K.; Eriste, E.; Langel, U. Cell-penetrating peptides: design, synthesis, and applications. *ACS Nano* **2014**, *8* (3), 1972–1994.
- (2) Hewitt, W. M.; Leung, S. S.; Pye, C. R.; Ponkey, A. R.; Bednarek, M.; Jacobson, M. P.; Lokey, R. S. Cell-permeable cyclic peptides from synthetic libraries inspired by natural products. *J. Am. Chem. Soc.* **2015**, *137* (2), 715–721.
- (3) Wang, C. K.; Northfield, S. E.; Colless, B.; Chaousis, S.; Hamernig, I.; Lohman, R. J.; Nielsen, D. S.; Schroeder, C. I.; Liras, S.; Price, D. A.; Fairlie, D. P.; Craik, D. J. Rational design and synthesis of an orally bioavailable peptide guided by NMR amide temperature coefficients. *Proc. Natl. Acad. Sci. U.S.A.* **2014**, *111* (49), 17504–17509.
- (4) Nielsen, D. S.; Hoang, H. N.; Lohman, R. J.; Hill, T. A.; Lucke, A. J.; Craik, D. J.; Edmonds, D. J.; Griffith, D. A.; Rotter, C. J.; Ruggeri, R. B.; Price, D. A.; Liras, S.; Fairlie, D. P. Improving on nature: making a cyclic heptapeptide orally bioavailable. *Angew. Chem., Int. Ed.* **2014**, *53* (45), 12059–12063.
- (5) Craik, D. J.; Fairlie, D. P.; Liras, S.; Price, D. The future of peptide-based drugs. *Chem. Biol. Drug Des.* **2013**, *81* (1), 136–147.
- (6) Millward, S. W.; Fiacco, S.; Austin, R. J.; Roberts, R. W. Design of cyclic peptides that bind protein surfaces with antibody-like affinity. *ACS Chem. Biol.* **2007**, *2* (9), 625–634.
- (7) Wessjohann, L. A.; Ruijter, E.; Garcia-Rivera, D.; Brandt, W. What can a chemist learn from nature's macrocycles? A brief, conceptual view. *Mol. Diversity* **2005**, *9* (1–3), 171–186.
- (8) Driggers, E. M.; Hale, S. P.; Lee, J.; Terrett, N. K. The exploration of macrocycles for drug discovery—an underexploited structural class. *Nat. Rev. Drug Discovery* **2008**, *7* (7), 608–624.
- (9) Dandapani, S.; Marcaurette, L. A. Grand challenge commentary: Accessing new chemical space for “undruggable” targets. *Nat. Chem. Biol.* **2010**, *6* (12), 861–863.
- (10) Villar, E. A.; Beglov, D.; Chennamadhavuni, S.; Porco, J. A., Jr.; Kozakov, D.; Vajda, S.; Whitty, A. How proteins bind macrocycles. *Nat. Chem. Biol.* **2014**, *10* (9), 723–731.
- (11) Lipinski, C. A.; Lombardo, F.; Dominy, B. W.; Feeney, P. J. Experimental and computational approaches to estimate solubility and

permeability in drug discovery and development settings. *Adv. Drug Delivery Rev.* **2001**, *46* (1–3), 3–26.

(12) Lipinski, C. A.; Lombardo, F.; Dominy, B. W.; Feeney, P. J. Experimental and computational approaches to estimate solubility and permeability in drug discovery and development settings. *Adv. Drug Delivery Rev.* **1997**, *23* (1–3), 3–25.

(13) Giordanetto, F.; Kihlberg, J. Macrocyclic drugs and clinical candidates: What can medicinal chemists learn from their properties? *J. Med. Chem.* **2014**, *57*, 278–295.

(14) Bockus, A. T.; McEwen, C. M.; Lokey, R. S. Form and function in cyclic peptide natural products: a pharmacokinetic perspective. *Curr. Top. Med. Chem.* **2013**, *13* (7), 821–836.

(15) White, T. R.; Renzelman, C. M.; Rand, A. C.; Rezai, T.; McEwen, C. M.; Gelev, V. M.; Turner, R. A.; Linington, R. G.; Leung, S. S.; Kalgutkar, A. S.; Bauman, J. N.; Zhang, Y.; Liras, S.; Price, D. A.; Mathiowetz, A. M.; Jacobson, M. P.; Lokey, R. S. On-resin N-methylation of cyclic peptides for discovery of orally bioavailable scaffolds. *Nat. Chem. Biol.* **2011**, *7* (11), 810–817.

(16) Ashwood, V. A.; Field, M. J.; Horwell, D. C.; Julien-Larose, C.; Lewthwaite, R. A.; McCleary, S.; Pritchard, M. C.; Raphy, J.; Singh, L. Utilization of an intramolecular hydrogen bond to increase the CNS penetration of an NK(1) receptor antagonist. *J. Med. Chem.* **2001**, *44* (14), 2276–2285.

(17) Over, B.; McCarren, P.; Artursson, P.; Foley, M.; Giordanetto, F.; Gronberg, G.; Hilgendorf, C.; Lee, M. D. t.; Matsson, P.; Muncipinto, G.; Pellisson, M.; Perry, M. W.; Svensson, R.; Duvall, J. R.; Kihlberg, J. Impact of stereospecific intramolecular hydrogen bonding on cell permeability and physicochemical properties. *J. Med. Chem.* **2014**, *57* (6), 2746–2754.

(18) Ettore, A.; D'Andrea, P.; Mauro, S.; Porcelloni, M.; Rossi, C.; Altamura, M.; Catalioto, R. M.; Giuliani, S.; Maggi, C. A.; Fattori, D. hNK2 receptor antagonists. The use of intramolecular hydrogen bonding to increase solubility and membrane permeability. *Bioorg. Med. Chem. Lett.* **2011**, *21* (6), 1807–1809.

(19) Wu, C.; Decker, E. R.; Blok, N.; Li, J.; Bourgoynne, A. R.; Bui, H.; Keller, K. M.; Knowles, V.; Li, W.; Stavros, F. D.; Holland, G. W.; Brock, T. A.; Dixon, R. A. Acyl substitution at the ortho position of anilides enhances oral bioavailability of thiophene sulfonamides: TBC3214, an ETA selective endothelin antagonist. *J. Med. Chem.* **2001**, *44* (8), 1211–1216.

(20) Sasaki, S.; Cho, N.; Nara, Y.; Harada, M.; Endo, S.; Suzuki, N.; Furuya, S.; Fujino, M. Discovery of a thieno[2,3-d]pyrimidine-2,4-dione bearing a p-methoxyureidophenyl moiety at the 6-position: a highly potent and orally bioavailable non-peptide antagonist for the human luteinizing hormone-releasing hormone receptor. *J. Med. Chem.* **2003**, *46* (1), 113–124.

(21) Rafi, S. B.; Hearn, B. R.; Vedantham, P.; Jacobson, M. P.; Renslo, A. R. Predicting and improving the membrane permeability of peptidic small molecules. *J. Med. Chem.* **2012**, *55* (7), 3163–3169.

(22) Rezai, T.; Bock, J. E.; Zhou, M. V.; Kalyanaraman, C.; Lokey, R. S.; Jacobson, M. P. Conformational flexibility, internal hydrogen bonding, and passive membrane permeability: successful in silico prediction of the relative permeabilities of cyclic peptides. *J. Am. Chem. Soc.* **2006**, *128* (43), 14073–14080.

(23) Rezai, T.; Yu, B.; Millhauser, G. L.; Jacobson, M. P.; Lokey, R. S. Testing the conformational hypothesis of passive membrane permeability using synthetic cyclic peptide diastereomers. *J. Am. Chem. Soc.* **2006**, *128* (8), 2510–2511.

(24) Yudin, A. K. Macrocycles: lessons from the distant past, recent developments, and future directions. *Chem. Sci.* **2015**, *6* (1), 30–49.

(25) Beck, J. G.; Chatterjee, J.; Laufer, B.; Kiran, M. U.; Frank, A. O.; Neubauer, S.; Ovadia, O.; Greenberg, S.; Gilon, C.; Hoffman, A.; Kessler, H. Intestinal permeability of cyclic peptides: common key backbone motifs identified. *J. Am. Chem. Soc.* **2012**, *134* (29), 12125–12133.

(26) Thansandote, P.; Harris, R. M.; Dexter, H. L.; Simpson, G. L.; Pal, S.; Upton, R. J.; Valko, K. Improving the passive permeability of macrocyclic peptides: balancing permeability with other physicochemical properties. *Bioorg. Med. Chem.* **2015**, *23* (2), 322–327.

(27) Klages, J.; Neubauer, C.; Coles, M.; Kessler, H.; Luy, B. Structure refinement of cyclosporin A in chloroform by using RDCs measured in a stretched PDMS-gel. *ChemBioChem* **2005**, *6* (9), 1672–1678.

(28) Kessler, H.; Gehrke, M.; Lautz, J.; Kock, M.; Seebach, D.; Thaler, A. Complexation and medium effects on the conformation of cyclosporin A studied by NMR spectroscopy and molecular dynamics calculations. *Biochem. Pharmacol.* **1990**, *40* (1), 169–173.

(29) Xu, Y.; Kersten, R. D.; Nam, S. J.; Lu, L.; Al-Suwailem, A. M.; Zheng, H.; Fenical, W.; Dorrestein, P. C.; Moore, B. S.; Qian, P. Y. Bacterial biosynthesis and maturation of the didemnin anti-cancer agents. *J. Am. Chem. Soc.* **2012**, *134* (20), 8625–8632.

(30) Masuoka, Y.; Nagai, A.; Shin-ya, K.; Furihata, K.; Nagai, K.; Suzuki, K.; Hayakawa, Y.; Seto, H. Spiruchostatins A and B, novel gene expression-enhancing substances produced by *Pseudomonas* sp. *Tetrahedron. Lett.* **2001**, *42* (1), 41–44.

(31) Yurek-George, A.; Habens, F.; Brimmell, M.; Packham, G.; Ganesan, A. Total synthesis of spiruchostatin A, a potent histone deacetylase inhibitor. *J. Am. Chem. Soc.* **2004**, *126* (4), 1030–1031.

(32) Linington, R. G.; Clark, B. R.; Trimble, E. E.; Almanza, A.; Urena, L. D.; Kyle, D. E.; Gerwick, W. H. Antimalarial peptides from marine cyanobacteria: isolation and structural elucidation of gallinamide A. *J. Nat. Prod.* **2009**, *72* (1), 14–17.

(33) Coleman, J. E.; Desilva, E. D.; Kong, F. M.; Andersen, R. J.; Allen, T. M. Cytotoxic peptides from the marine sponge *Cymbastela* sp. *Tetrahedron* **1995**, *51* (39), 10653–10662.

(34) Walsh, C. T.; O'Brien, R. V.; Khosla, C. Nonproteinogenic amino acid building blocks for nonribosomal peptide and hybrid polyketide scaffolds. *Angew. Chem., Int. Ed.* **2013**, *52* (28), 7098–7124.

(35) Tan, L. T.; Okino, T.; Gerwick, W. H. Bouillonamide: a mixed polyketide-peptide cytotoxin from the marine cyanobacterium *Moorea bouillonii*. *Mar. Drugs* **2013**, *11* (8), 3015–3024.

(36) Hill, T. A.; Shepherd, N. E.; Diness, F.; Fairlie, D. P. Constraining cyclic peptides to mimic protein structure motifs. *Angew. Chem., Int. Ed.* **2014**, *53* (48), 13020–13041.

(37) Hagihara, M.; Anthony, N.; Stout, T.; Clardy, J.; Schreiber, S. Vinylogous polypeptides—an alternative peptide backbone. *J. Am. Chem. Soc.* **1992**, *114* (16), 6568–6570.

(38) Guimaraes, C. R.; Mathiowetz, A. M.; Shalaeva, M.; Goetz, G.; Liras, S. Use of 3D properties to characterize beyond rule-of-5 property space for passive permeation. *J. Chem. Inf. Model.* **2012**, *52* (4), 882–890.

(39) Ovadia, O.; Greenberg, S.; Chatterjee, J.; Laufer, B.; Opperer, F.; Kessler, H.; Gilon, C.; Hoffman, A. The effect of multiple N-methylation on intestinal permeability of cyclic hexapeptides. *Mol. Pharmacol.* **2011**, *8* (2), 479–487.

(40) Marzinzik, A. L.; Vorherr, T. E. Towards intracellular delivery of peptides. *Chimia* **2013**, *67* (12–13), 899–904.

(41) Bock, J. E.; Gavenonis, J.; Kritzer, J. A. Getting in shape: controlling peptide bioactivity and bioavailability using conformational constraints. *ACS Chem. Biol.* **2013**, *8* (3), 488–499.

(42) Wahyudi, H.; Tantisantisom, W.; Liu, X.; Ramsey, D. M.; Singh, E. K.; McAlpine, S. R. Synthesis, structure-activity analysis, and biological evaluation of sanguinamide B analogues. *J. Org. Chem.* **2012**, *77* (23), 10596–10616.

(43) Alex, A.; Millan, D. S.; Perez, M.; Wakenhut, F.; Whitlock, G. A. Intramolecular hydrogen bonding to improve membrane permeability and absorption in beyond rule of five chemical space. *MedChemComm* **2011**, *2* (7), 669–674.

(44) Nielsen, D. S.; Hoang, H. N.; Lohman, R. J.; Diness, F.; Fairlie, D. P. Total synthesis, structure, and oral absorption of a thiazole cyclic peptide, sanguinamide A. *Org. Lett.* **2012**, *14* (22), 5720–5723.

(45) Biron, E.; Chatterjee, J.; Ovadia, O.; Langenegger, D.; Bruegggen, J.; Hoyer, D.; Schmid, H. A.; Jelinek, R.; Gilon, C.; Hoffman, A.; Kessler, H. Improving oral bioavailability of peptides by multiple N-methylation: somatostatin analogues. *Angew. Chem., Int. Ed.* **2008**, *47* (14), 2595–2599.



- (46) Chatterjee, J.; Mierke, D. F.; Kessler, H. Conformational preference and potential templates of N-methylated cyclic pentaalane peptides. *Chemistry* **2008**, *14* (5), 1508–1517.
- (47) Schwochert, J.; Pye, C.; Ahlback, C.; Abdollahian, Y.; Farley, K.; Khunte, B.; Limberakis, C.; Kalgutkar, A. S.; Eng, H.; Shapiro, M. J.; Mathiowetz, A. M.; Price, D. A.; Liras, S.; Lokey, R. S. Revisiting N-to-O acyl shift for synthesis of natural product-like cyclic depsipeptides. *Org. Lett.* **2014**, *16* (23), 6088–6091.
- (48) Zaretsky, S.; Scully, C. C.; Lough, A. J.; Yudin, A. K. Exocyclic control of turn induction in macrocyclic peptide scaffolds. *Chemistry* **2013**, *19* (52), 17668–17672.
- (49) Hwang, S.-H.; Blaskovich, M. A.; Kim, H.-O. A convenient reduction of alpha-amino acids to 1,2-amino alcohols with retention of optical purity. *Open Org. Chem. J.* **2008**, *2*, 107–109.
- (50) Gilles, A.; Martinez, J.; Cavalier, F. Supported synthesis of oxoapratoxin A. *J. Org. Chem.* **2009**, *74* (11), 4298–4304.
- (51) Freidinger, R. M.; Hinkle, J. S.; Perlow, D. S.; Arison, B. H. Synthesis of 9-fluorenylmethoxycarbonyl-protected n-alkyl amino-acids by reduction of oxazolidinones. *J. Org. Chem.* **1983**, *48* (1), 77–81.
- (52) Cadicamo, C. D.; Asante, V.; Abu Ammar, M.; Borelli, C.; Korting, H. C.; Kokscho, B. Investigation of the synthetic route to pepstatin analogues by SPPS using O-protected and O-unprotected statine as building blocks. *J. Pept. Sci.* **2009**, *15* (4), 272–277.
- (53) Kansy, M.; Senner, F.; Gubernator, K. Physicochemical high throughput screening: parallel artificial membrane permeation assay in the description of passive absorption processes. *J. Med. Chem.* **1998**, *41* (7), 1007–1010.
- (54) Avdeef, A. *Absorption and Drug Development: Solubility, Permeability, and Charge State*, 2nd ed.; Wiley & Sons, Inc.: Hoboken, NJ, 2012.
- (55) Leung, S. S.; Mijalkovic, J.; Borrelli, K.; Jacobson, M. P. Testing physical models of passive membrane permeation. *J. Chem. Inf. Model.* **2012**, *52* (6), 1621–1636.
- (56) Di, L.; Whitney-Pickett, C.; Umland, J. P.; Zhang, H.; Zhang, X.; Gebhard, D. F.; Lai, Y.; Federico, J. J., 3rd; Davidson, R. E.; Smith, R.; Reyner, E. L.; Lee, C.; Feng, B.; Rotter, C.; Varma, M. V.; Kempshall, S.; Fenner, K.; El-Kattan, A. F.; Liston, T. E.; Troutman, M. D. Development of a new permeability assay using low-efflux MDCKII cells. *J. Pharm. Sci.* **2011**, *100* (11), 4974–4985.
- (57) Fukushima, K.; Shibata, M.; Mizuhara, K.; Aoyama, H.; Uchisako, R.; Kobuchi, S.; Sugioka, N.; Takada, K. Effect of serum lipids on the pharmacokinetics of atazanavir in hyperlipidemic rats. *Biomed. Pharmacother.* **2009**, *63* (9), 635–642.
- (58) Lombardo, F.; Shalaeva, M. Y.; Tupper, K. A.; Gao, F. ElogDoct: A tool for lipophilicity determination in drug discovery. 2. Basic and neutral compounds. *J. Med. Chem.* **2001**, *44* (15), 2490–2497.
- (59) Goetz, G. H.; Farrell, W.; Shalaeva, M.; Sciabola, S.; Anderson, D.; Yan, J.; Philippe, L.; Shapiro, M. J. High throughput method for the indirect detection of intramolecular hydrogen bonding. *J. Med. Chem.* **2014**, *57* (7), 2920–2929.
- (60) Goetz, G. H.; Philippe, L.; Shapiro, M. J. EPSA: A novel supercritical fluid chromatography technique enabling the design of permeable cyclic peptides. *ACS Med. Chem. Lett.* **2014**, *5* (10), 1167–1172.
- (61) Butts, C. P.; Jones, C. R.; Harvey, J. N. High precision NOEs as a probe for low level conformers—a second conformation of strychnine. *Chem. Commun. (Cambridge, U. K.)* **2011**, *47* (4), 1193–1195.
- (62) Butts, C. P.; Jones, C. R.; Towers, E. C.; Flynn, J. L.; Appleby, L.; Barron, N. J. Interproton distance determinations by NOE—surprising accuracy and precision in a rigid organic molecule. *Org. Biomol. Chem.* **2011**, *9* (1), 177–184.
- (63) Jacobson, M. P.; Pincus, D. L.; Rapp, C. S.; Day, T. J.; Honig, B.; Shaw, D. E.; Friesner, R. A. A hierarchical approach to all-atom protein loop prediction. *Proteins* **2004**, *55* (2), 351–367.
- (64) Atasoylu, O.; Furst, G.; Risatti, C.; Smith, A. B., 3rd. The solution structure of (+)-spongistatin 1 in DMSO. *Org. Lett.* **2010**, *12* (8), 1788–1791.
- (65) Lai, X. N.; Chen, C. P.; Andersen, N. H. The discon algorithm, an accurate and robust alternative to an eigenvalue solution for extracting experimental distances from noesy data. *J. Magn. Reson. B* **1993**, *101* (3), 271–288.
- (66) Qu, Z. W.; Zhu, H.; May, V. Unambiguous assignment of vibrational spectra of cyclosporin A and H. *J. Phys. Chem. A* **2010**, *114* (36), 9768–9773.
- (67) In, Y.; Ishida, T.; Takesako, K. Unique molecular conformation of aureobasidin A, a highly amide N-methylated cyclic depsipeptide with potent antifungal activity: X-ray crystal structure and molecular modeling studies. *J. Pept. Res.* **1999**, *53* (5), 492–500.
- (68) Searle, M. S.; Hall, J. G.; Wakelin, P. G. <sup>1</sup>H- and <sup>13</sup>C-n.m.r. studies of the antitumour antibiotic luzopeptin. Resonance assignments, conformation and flexibility in solution. *Biochem. J.* **1988**, *256* (1), 271–278.
- (69) Amagata, T.; Morinaka, B. I.; Amagata, A.; Tenney, K.; Valeriote, F. A.; Lobkovsky, E.; Clardy, J.; Crews, P. A chemical study of cyclic depsipeptides produced by a sponge-derived fungus. *J. Nat. Prod.* **2006**, *69* (11), 1560–1565.
- (70) Jin, M.; Shimada, T.; Shintani, M.; Yokogawa, K.; Nomura, M.; Miyamoto, K. Long-term levothyroxine treatment decreases the oral bioavailability of cyclosporin A by inducing P-glycoprotein in small intestine. *Drug Metab. Pharmacokinet.* **2005**, *20*, 324–330.